

# Cirrus cloud thinning using a more physically-based ice microphysics scheme in the ECHAM-HAM GCM (acp-2021-685)

Colin Tully, David Neubauer, Nadja Omanovic, and Ulrike Lohmann  
25<sup>th</sup> May 2022

## Author Responses

Dear Prof. Liu

On behalf of all coauthors, I would like to thank you for serving as the editor of our submission and considering it for publication in ACP. I would also like to thank the reviewers for their useful comments on improvements to our study. Please find our author responses to the second round of reviews from Referees #4 and #3.

Sincerely,  
Colin Tully

### Response to Referee #4

1. **Comment:** Do the authors know why there is a relatively large discrepancy between the model and observations between the 215 to 250 K range for low ICNC in Figure 2?
  - a. **Response:** Yes, we believe this is due to the fact that we compare five-year annual mean model data to instantaneous observational data. We added text in the manuscript to describe this specifically
  - b. **Changes in the text at lines 343-346:**

*“... The model also does not capture the wide variability of ICNC values as seen in the in-situ measurements, as like the higher frequency of low ICNC values between roughly 205 K and 250 K. This is due to the fact that we compare five-year annual mean model data to instantaneous values recorded during various aircraft campaigns. ...”*

2. **Comment:** please include justification of choice for  $S_{i,seed}$ =1.05 and 1.35 in the manuscript itself
  - a. **Response:** We included explicit justification for our choice of  $S_{i,seed}$  values in the revised manuscript
  - b. **Changes in the text at lines: 290-297:**

*“The  $S_{i,seed}$  of 1.05 follows Storelvmo and Herger (2014) and Gasparini and Lohmann (2016), and is based on suggestions of a hypothetical, highly-efficient seeding particle material. However, it is unclear whether this  $S_{i,seed}$  can be applied to a realistic seeding particle material. Mitchell and Finnegan (2009) suggested bismuth tri-iodide, but the specific ice nucleating properties of this material are unknown. Therefore, to test the sensitivity of ice nucleation competition to  $S_{i,seed}$ , we conducted additional seeding simulations with all seeding particle concentrations described above, with a  $S_{i,seed}$  of 1.35 (Table 3). We chose this relatively high  $S_{i,seed}$  value to ensure that seeding can occur in ice supersaturated*

*environments below the lower homogeneous nucleation  $S_{i,crit}$  threshold roughly  $\geq 1.40$  and, in order to be less competitive with background heterogeneous nucleation processes, above the maximum  $S_{i,crit}$  for dust of 1.3.”*

3. **Comment:** one new comment: Lines 198-201 and lines 207-211 of the version of the manuscript with tracked changes: If water vapour consumption by ice crystal growth is accounted for as a sink of supersaturation, then why does an artificial downdraft need to be introduced in the model at the end of each time step?
  - a. **Response:** Supersaturation in our cirrus model can only be updated through changes to the updraft velocity. Therefore, in order to quantify the effect of water vapor consumption, a fictitious downdraft is introduced to counteract the updraft. We expanded our explanation in the text to make this discussion clearer:
  - b. **Changes in the text at lines 187-215:**

*“A separate scheme by Kärcher et al. (2006) that was adapted for ECHAM-HAM by Kuebbeler et al. (2014) handles in-situ ice nucleation within cirrus clouds. It simulates the competition for water vapor between heterogeneous and homogeneous nucleation, and between depositional growth onto pre-existing ice particles that are transported into the cirrus regime from 190 deep convective detrainment or from stratiform mixed-phase clouds. The scheme uses a sub-stepping approach to simulate the temporal evolution of ice saturation ratio ( $S_i$ ) in an air parcel rising adiabatically during the formation-stage of a cirrus cloud. Ice formation occurs only when  $S_i$  reaches the critical values for heterogeneous or homogeneous nucleation (see below). The evolution of  $S_i$  is determined by the balance between the adiabatic cooling rate of rising air and the diffusional growth of ice particles that consume the available water vapor. As the cooling rate, and therefore the magnitude of  $S_i$ , is directly related to the strength of vertical velocity, a fictitious downdraft that counteracts the vertical velocity is introduced at the start of each timestep of the cirrus sub-model to quantify the effect of water vapor consumption onto pre-existing ice particles, which includes new ice formation in the previous cirrus sub-model timestep (Kuebbeler et al., 2014). This “effective vertical velocity” (updraft + fictitious downdraft), therefore, determines the magnitude of  $S_i$ , and is calculated at the end of a single sub-timestep of the cirrus scheme. It is used in the subsequent sub-timestep to update  $S_i$ .*

*Vertical velocity is represented by a grid-mean value plus a turbulent component based on the turbulent kinetic energy (TKE), (Brinkop and Roeckner, 1995; Kuebbeler et al., 2014). Orographic effects on vertical velocity as well as small-scale gravity waves (Kärcher et al., 2006; Joos et al., 2008, 2010; Jensen et al., 2016a) in the upper troposphere are not included in this study. We provide a short analysis that verifies our model without orographic effects in Appendix A. In summary, by using the new P3 ice microphysics and the updated cirrus ice nucleation schemes, including orographic effects acts to drastically increase cirrus ICNC while reducing spatial heterogeneity. Muench and Lohmann (2020) updated the water vapor consumption by ice, following the diffusional growth equation (Lohmann et al., 2016). The temporal change of the saturation ratio follows such that if the updraft is stronger than the water vapor consumption by pre-existing ice and heterogeneous INPs, then it may reach a suitable magnitude for homogeneous nucleation to occur. The opposite is true in weaker updraft regimes or in high INP concentration environments (Kärcher et al., 2006). The sub-stepping approach in the cirrus scheme is computed dynamically based on a 1 % rate of change of the ice saturation ratio between each sub-timestep.”*

### Response to Referee #3

I am sending you this letter in response to one reviewer who does not concur with the exclusion of orographic-induced gravity waves in our model. In summary, we do not agree with the statements in their response to our rebuttal that was submitted with the revised manuscript in March 2022. We refer to the original rebuttal as the basis for understanding our stance on this issue and provide additional data in this letter to support our argument.

The motivation behind our study is to re-evaluate the relatively new climate intervention proposal, cirrus cloud thinning (CCT), after improvements were made to the representation of ice microphysics in our model. Firstly, we use the Predicted Particle Properties (P3) ice microphysics scheme by Morrison and Milbrandt (2015) that was ported to ECHAM6 by Dietlicher et al. (2018, 2019). The scheme represents the ice population under a single prognostic category, instead of differentiating between in-cloud and precipitating ice like in the default ECHAM6 two-moment (2M) microphysics scheme by Lohmann et al. (2007). In the 2M scheme, once cloud ice grew to a certain size, it was transferred to the snow category and would reach the surface within one model timestep. To maintain radiative balance within the modeled climate, this conversion from cloud-ice to snow was greatly enhanced (Neubauer et al., 2019), thus artificially accelerating ice removal. This is no longer the case using P3, and, as we note in the manuscript, this impacts the lifetime of ice within clouds, which has subsequent effects on cloud fractions and radiative properties. Secondly, our cloud microphysics scheme is coupled to a separate cirrus ice formation scheme based on Kärcher et al. (2006) and Kuebbeler et al. (2014), with updates to the code made by Muench and Lohmann (2020), including using the water vapor deposition equation by Lohmann et al. (2016). The scheme simulates the competition for available water vapor between pre-existing ice, heterogeneous nucleation onto mineral dust particles, and homogeneous nucleation of liquid sulfate aerosols. We made an additional improvement, which is described in the manuscript, that addressed the overestimation of the number of aerosols that previously nucleated ice. Finally, in our study we assess the sensitivity of CCT to the choice of relative humidity-based cloud fraction parameterizations, using the default Sundqvist et al. (1989), (S89) scheme and the updated scheme by Dietlicher et al. (2019), (D19). S89 represents ice cloud fraction analogously to liquid cloud such that at ice saturation, a cirrus cloud fully covers a gridbox. As ice supersaturation is required for ice formation and newly formed cirrus will not necessarily cover the entire coarse resolution of a model gridbox (roughly 160 km x 160 km), we use D19 that allows for partial cirrus cloud gridbox coverage above ice saturation. Therefore, we argue that, cumulatively, these updates made to our model lead to a more physically-based representation of ice microphysics that lends itself to a reassessment of CCT. In the following we provide additional data to discuss the exclusion of the orographic gravity wave component of the vertical velocity based on our specific model setup described above. We cover a comparison to the in-situ data by Krämer et al. (2020) and a discussion on the turbulent vertical velocity in our model.

As you may have read in our original rebuttal, we did not activate the orographic gravity wave parameterization by Joos et al. (2008, 2010) in the first instance as in initial tests we believed we were double counting the turbulent kinetic energy (TKE) and orographic components of the vertical velocity in grid cells where orography was active. This resulted in high ice crystal number concentration (ICNC) values that did not provide us with confidence in our results. It turned out this was not the case and was merely due to a numerical issue, related to parallelization, when using the parameterization in ECHAM6.3 with the P3 ice microphysics scheme. After reworking the code to make it compatible with P3, we could easily include this vertical velocity component in our simulations. However, after re-running our reference simulation (Full\_D19 of the manuscript) to verify this new approach, we found that including the orographic component worsens the model agreement with in-situ observations as well as with satellite retrievals of cirrus clouds at increasingly colder temperatures (see our original rebuttal).

We validated our model using the in-situ measurements by Krämer et al. (2020), (K20). Figure 1 shows the model validation comparison between our original model that is presented in the manuscript (P3 Ref) and the revised model including the orographic velocity component (P3 Oro) for the reference, Full\_D19, simulation. This figure is now included in Appendix A of the revised manuscript. The most notable feature we find with P3 Oro is the large increase in ICNC between roughly 200 K and 220 K in Figure 1a. The largest difference is at 202 K, where ICNC increased by over two orders of magnitude compared to P3 Ref. There is a similar magnitude of discrepancy between the K20 data and P3 Oro. With the orographic velocity component, the model predicts high frequencies (near 100 %) of ICNC around 2000 L<sup>-1</sup>. Such values in the K20 data (Figure 1c) and P3 Ref (Figure 1b) have a frequency of less than 1%. We note that P3 Ref and P3 Oro show much less variability than the K20 data as they are averaged over five years, whereas the aircraft data are instantaneous. However, we also note that P3 Ref shows excellent agreement in median ICNC values with the K20 data that is not evident for colder cirrus clouds with P3 Oro.

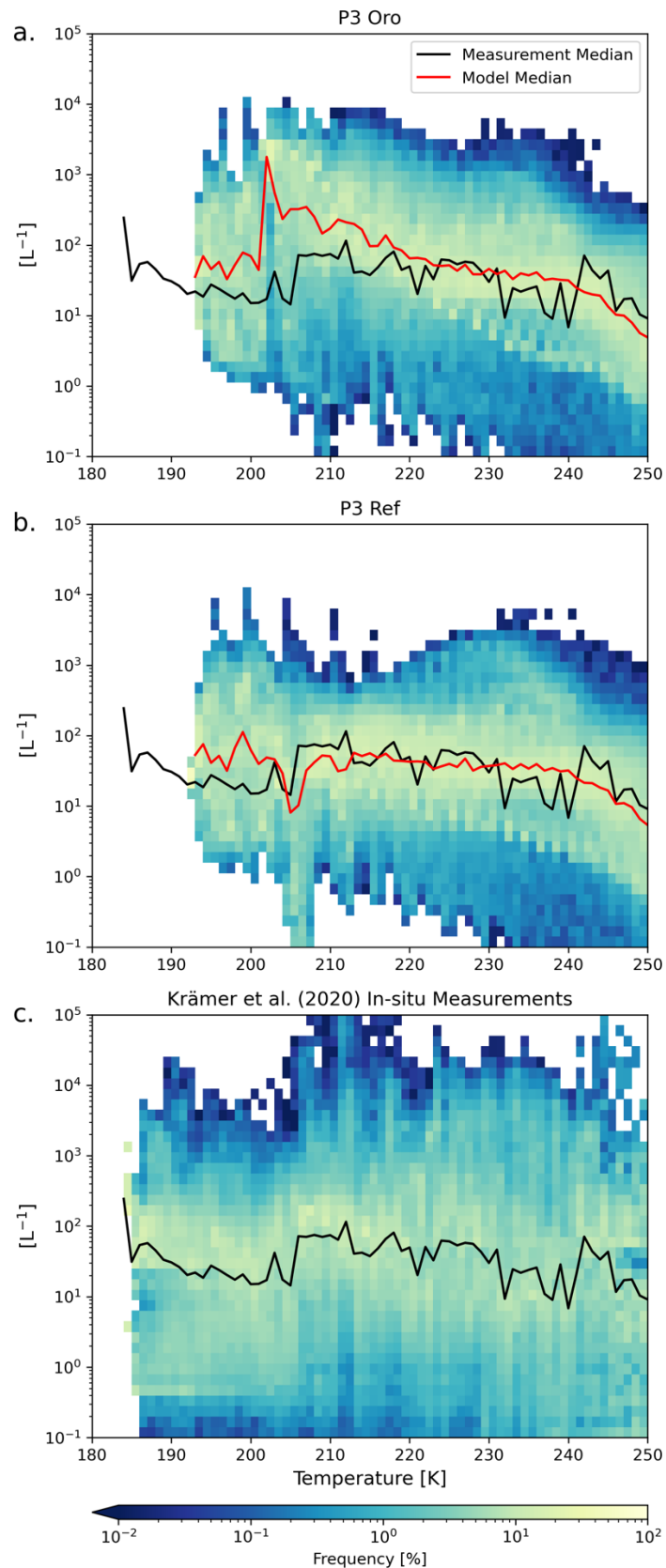


Figure 1: ICNC frequency diagrams for ice crystals with a diameter of at least  $3 \mu\text{m}$  as a function of temperature between 180 K and 250 K binned like in Krämer et al. (2020) for every 1 K for (a.) P3 with the orographic velocity component (P3 Oro), (b.) without the orographic velocity component (P3 Ref), and (c.) the in-situ flight data from Krämer et al. (2020). The red line in the upper two plots represents the binned median ICNC value of the model data, and the black line in all plots is the same value for the observational data.

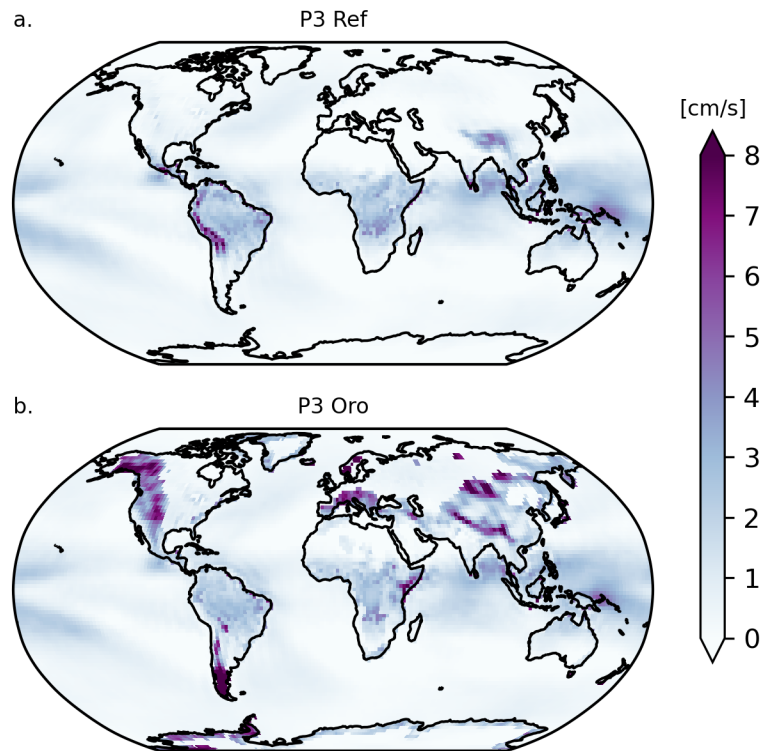


Figure 2: Five-year annual mean spatial distribution of the total as calculated in the P3 ice microphysics scheme and sent to the cirrus ice nucleation scheme on the 200 hPa level for (a.) P3 Ref without the orographic velocity component activated and (b.) P3 Oro with the orographic component of the vertical velocity activated.

Vertical motions in ECHAM6.3 are computed from the sum of a grid mean vertical velocity and a turbulent component based on the turbulent kinetic energy (TKE) parameterization by Brinkop and Roeckner (1995), (Stevens et al., 2013; Neubauer et al., 2019). The scheme allows for the momentum transport either horizontally or vertically via turbulent diffusion. Above cloud layers, turbulence is formed as a result of longwave cloud-top cooling. When the orographic gravity wave parameterization is activated as in P3 Oro, the turbulent component of the vertical velocity is computed such that TKE and orographic gravity-waves do not overlap spatially, i.e. turbulent effects are not double-counted within model gridboxes. Figure 2 presents the total vertical velocity for P3 Ref (a) and P3 Oro (b) on the 200 hPa level that is used as input to the cirrus ice nucleation scheme (Section 2 of the main text). The orographic gravity wave component has a clear impact on the total vertical velocity as expected over mountain ranges such as the Rockies, the European Alps, and the Himalayas. It is unclear why the orographic component is less prominent over the northern Andes in our model, but rather leads to a shift towards southern high latitudes. We also note positive vertical velocity impacts over high-terrain regions such as Greenland and the Antarctic Peninsula when activating the orographic scheme. Positive vertical velocity changes of more than 8 cm/s as seen in Figure 2 greatly impact the formation environment of ice crystals within cirrus clouds. Kärcher and Lohmann (2002) developed a theoretical framework for simulating homogeneous freezing within young cirrus, which serves as the basis of the cirrus ice nucleation scheme used in our model (Kärcher et al., 2006; Kuebbeler

et al., 2014; Muench and Lohmann, 2020). They showed that the number of ice particles resulting from a homogeneous nucleation event is rather insensitive to the particle size distribution, but instead is highly dependent on the strength of the updraft, with higher sensitivity for increasingly lower temperatures. Jensen et al. (2016) also found a direct relationship between the number of ice crystals formed by homogeneous nucleation and updraft strength. The behavior we find in our model when activating the orographic gravity wave component is consistent with these theoretical frameworks. The large median ICNC increase we find with P3 Oro at 202 K compared to P3 Ref and the in-situ observations by Krämer et al. (2020) in Figure 1 is the direct result of more frequent homogeneous nucleation in our cirrus scheme in response to stronger vertical velocities. While our model follows directly from theory, this enhancement of the number of ice particles forming in cirrus clouds with the orographic component activated, worsens model agreement with observations.

We argue that the orographic gravity wave parameterization by Joos et al. (2008, 2010) in its current form is incompatible with ECHAM6.3 when using the P3 ice microphysics scheme. While we accept that including physical processes controlling ice hydrometeor populations is vital to understanding their impacts on cloud properties, the inclusion of additional parameterizations should only be included if they improve our representation of climate system. Based on our findings in the manuscript, our original rebuttal, and what we presented in this letter, the orographic gravity wave velocity parameterization requires additional validation when coupled to P3, which exceeds the scope of this study. We extended the appendix in the revised manuscript to include the figures and the text provided in this response. You will see those changes as well as our adaptations to the Appendix in the tracked changes PDF.

## References

- Brinkop, S. and Roeckner, E.: Sensitivity of a general circulation model to parameterizations of cloud–turbulence interactions in the atmospheric boundary layer, *Tellus A*, 47, 197–220, <https://doi.org/10.1034/j.1600-0870.1995.t01-1-00004.x>, <https://onlinelibrary.wiley.com/doi/abs/10.1034/j.1600-0870.1995.t01-1-00004.x>, 1995.
- Dietlicher, R., Neubauer, D., and Lohmann, U.: Prognostic parameterization of cloud ice with a single category in the aerosol–climate model ECHAM(v6.3.0)-HAM(v2.3), *Geoscientific Model Development*, 11, 1557–1576, <https://doi.org/10.5194/gmd-11-1557-2018>, <https://gmd.copernicus.org/articles/11/1557/2018/>, 2018.
- Dietlicher, R., Neubauer, D., and Lohmann, U.: Elucidating ice formation pathways in the aerosol–climate model ECHAM6-HAM2, *Atmospheric Chemistry and Physics*, 19, 9061–9080, <https://doi.org/10.5194/acp-19-9061-2019>, <https://www.atmos-chem-phys.net/19/9061/2019/>, 2019.
- Jensen, E. J., Ueyama, R., Pfister, L., Bui, T. V., Lawson, R. P., Woods, S., Thornberry, T., Rollins, A. W., Diskin, G. S., DiGangi, J. P., and Avery, M. A.: On the Susceptibility of Cold Tropical Cirrus to Ice Nuclei Abundance, *Journal of the Atmospheric Sciences*, 73, 2445–2464, <https://doi.org/10.1175/JAS-D-15-0274.1>, <https://doi.org/10.1175/JAS-D-15-0274.1>, 2016.

- Joos, H., Spichtinger, P., and Lohmann, U.: Orographic cirrus in the global climate model ECHAM5, *Journal of Geophysical Research*, 113, <https://doi.org/10.1029/2007JD009605>, <https://agupubs.onlinelibrary.wiley.com/doi/abs/10.1029/2007JD009605>, 2008.
- Joos, H., Spichtinger, P., and Lohmann, U.: Influence of a future climate on the microphysical and optical properties of orographic cirrus clouds in ECHAM5, *Journal of Geophysical Research: Atmospheres*, 115, <https://doi.org/https://doi.org/10.1029/2010JD013824>, <https://agupubs.onlinelibrary.wiley.com/doi/abs/10.1029/2010JD013824>, 2010.
- Kärcher, B. and Lohmann, U.: A parameterization of cirrus cloud formation: Homogeneous freezing of supercooled aerosols, *Journal of Geophysical Research: Atmospheres*, 107, AAC 4–1–AAC 4–10, <https://doi.org/10.1029/2001JD000470>, <https://agupubs.onlinelibrary.wiley.com/doi/abs/10.1029/2001JD000470>, 2002.
- Kärcher, B., Hendricks, J., and Lohmann, U.: Physically based parameterization of cirrus cloud formation for use in global atmospheric models, *Journal of Geophysical Research: Atmospheres*, 111, <https://doi.org/10.1029/2005JD006219>, <https://agupubs.onlinelibrary.wiley.com/doi/abs/10.1029/2005JD006219>, 2006.
- Krämer, M., Rolf, C., Spelten, N., Afchine, A., Fahey, D., Jensen, E., Khaykin, S., Kuhn, T., Lawson, P., Lykov, A., Pan, L. L., Riese, M., Rollins, A., Stroh, F., Thornberry, T., Wolf, V., Woods, S., Spichtinger, P., Quaas, J., and Sourdeval, O.: A microphysics guide to cirrus – Part 2: Climatologies of clouds and humidity from observations, *Atmospheric Chemistry and Physics*, 20, 12 569–12 608, <https://doi.org/10.5194/acp-20-12569-2020>, <https://acp.copernicus.org/articles/20/12569/2020/>, 2020.
- Kuebbeler, M., Lohmann, U., Hendricks, J., and Kärcher, B.: Dust ice nuclei effects on cirrus clouds, *Atmospheric Chemistry and Physics*, 14, 3027–3046, <https://doi.org/10.5194/acp-14-3027-2014>, <https://www.atmos-chem-phys.net/14/3027/2014/>, 2014.
- Lohmann, U., Stier, P., Hoose, C., Ferrachat, S., Kloster, S., Roeckner, E., and Zhang, J.: Cloud microphysics and aerosol indirect effects in the global climate model ECHAM5-HAM, *Atmospheric Chemistry and Physics*, 7, 3425–3446, <https://doi.org/10.5194/acp-7-3425-2007>, <https://www.atmos-chem-phys.net/7/3425/2007/>, 2007.
- Lohmann, U., Lüönd, F., and Mahrt, F.: An Introduction to Clouds: From the Microscale to Climate, Cambridge University Press, <https://doi.org/10.1017/CBO9781139087513>, 2016.
- Morrison, H. and Milbrandt, J. A.: Parameterization of Cloud Microphysics Based on the Prediction of Bulk Ice Particle Properties. Part I: Scheme Description and Idealized Tests, *Journal of the Atmospheric Sciences*, 72, 287–311, <https://doi.org/10.1175/JAS-D-14-0065.1>, <https://doi.org/10.1175/JAS-D-14-0065.1>, 2015.
- Muench, S. and Lohmann, U.: Developing a Cloud Scheme With Prognostic Cloud Fraction and Two Moment Microphysics for ECHAM- HAM, *Journal of Advances in Modeling Earth Systems*, 12, e2019MS001 824, <https://doi.org/10.1029/2019MS001824>, <https://agupubs.onlinelibrary.wiley.com/doi/abs/10.1029/2019MS001824> , e2019MS001824 2019MS001824, 2020.
- Neubauer, D., Ferrachat, S., Siegenthaler-Le Drian, C., Stier, P., Partridge, D. G., Tegen, I., Bey, I., Stanelle, T., Kokkola, H., and Lohmann, U.: The global aerosol–climate model ECHAM6.3–HAM2.3 – Part 2: Cloud evaluation, aerosol radiative forcing, and climate sensitivity, *Geoscientific Model Development*, 12, 3609–3639,



<https://doi.org/10.5194/gmd-12-3609-2019>, <https://gmd.copernicus.org/articles/12/3609/2019/>, 2019.

- Stevens, B., Giorgetta, M., Esch, M., Mauritsen, T., Crueger, T., Rast, S., Salzmann, M., Schmidt, H., Bader, J., Block, K., Brokopf, R., Fast, I., Kinne, S., Kornblueh, L., Lohmann, U., Pincus, R., Reichler, T., and Roeckner, E.: Atmospheric component of the MPI-M Earth System Model: ECHAM6, *Journal of Advances in Modeling Earth Systems*, 5, 146–172, <https://doi.org/10.1002/jame.20015>, <https://agupubs.onlinelibrary.wiley.com/doi/abs/10.1002/jame.20015>, 2013.
- Sundqvist, H., Berge, E., and Kristjánsson, J. E.: Condensation and Cloud Parameterization Studies with a Mesoscale Numerical Weather Prediction Model, *Monthly Weather Review*, 117, 1641–1657, [https://doi.org/10.1175/1520-0493\(1989\)117<1641:CACPSW>2.0.CO;2](https://doi.org/10.1175/1520-0493(1989)117<1641:CACPSW>2.0.CO;2), 1989.